EPJ Web of Conferences **114**, 02022 (2016)
DOI: 10.1051/epjconf/201611402022

A non-intrusive and continuous-in-space technique to investigate the wave transformation and breaking over a breakwater

Simone Ferrari[1,a], Maria Grazia Badas[1] and Giorgio Querzoli[1]

[1]*DICAAR - Dipartimento di Ingegneria Civile, Ambientale e Architettura, University of Cagliari,via Marengo 2, 09123 Cagliari, Italy*

Abstract. To design longshore breakwaters, the evaluation of the wave motion transformations over the structures and of the energy they are able to absorb, dissipate and reflect is necessary. To characterize features and transformations of monochromatic wave trains above a breakwater, both submerged and emerged, we have designed and developed a non-intrusive and continuous-in-space technique, based on Image Analysis, and carried out an experimental campaign, in a laboratory flume equipped with a wave-maker, in order to test it. The investigation area was lighted with a light sheet and images were recorded by a video-camera. The working fluid was seeded with non buoyant particles to make it bright and clearly distinct from dark background and breakwater. The technique, that is based on a robust algorithm to identify the free surface, has showed to properly work also in prohibitive situations for traditional resistive probes (e.g., very shallow waters and/or breaking waves) and to be able to measure the free surface all over the investigation field in a non-intrusive way. Two kind of analysis were mainly performed, a statistical and a spectral one. The peculiarities of the measurement technique allowed to describe the whole wave transformation and to supply useful information for design purposes.

1 Introduction

Longshore breakwaters are extensively used as littoral or harbour protection systems (see, for instance, [1]) but also, more recently, as devices for wave energy conversion ([2]). As a consequence, the estimation of the wave motion transformations over the breakwater and of the amount of energy this structure is able to absorb, dissipate and reflect, is necessary, as stated in [3]. For instance, the proper design of longshore breakwaters for littoral protection requires that wave motion in the sheltered area is within certain limits, so laboratory experiments can be carried out to determine reflection and dissipation of the energy of trains of monochromatic waves above a breakwater, as in [4]. Unfortunately, the traditional instruments employed for this kind of experiments, i.e. the classical resistive probes (e.g., see [5]), can successfully measure water level on the lee and weather side of the breakwater but are not able to properly work above and close to it, where the water level is very shallow and the waves are possibly breaking. As a consequence, using traditional probes the breakwater results as a "black box" and it is not possible a direct comprehension of the physical phenomena determining the wave evolutions.

To overcome these issues, we have designed and developed a non-intrusive and continuous-in-space technique, based on Image Analysis, and carried out an experimental campaign, in a laboratory flume equipped with a wave-maker, in order to test it.

2 Experiments and data elaboration

The experimental campaign was carried out in the 21-m long flume (see Figure 1) of the Hydraulic Laboratory of the DICAAR – University of Cagliari. The flume has glass walls and it is equipped on one side with a wave-maker and on the opposite side with an absorbing beach, designed in order to minimise the reflection of the incoming waves. The wave-maker is controlled by a pc and this system is able to generate both monochromatic regular wave trains or random waves from a given spectrum. More details on the flume and the wave-maker can be found in Ferrari and Querzoli, 2015 [6].

The model breakwater employed in this experimental campaign was a black painted trapezoidal obstacle made of Perspex: it is 26.0 cm height, with a lower side 124.0 cm long, an upper side 20.0 cm long and a cross section 30.0 cm wide (same width as the flume). As breakwaters for littoral protection or for energy conversion can be both submerged or emerged, the hydrostatic level in the experiments was of 29.0, 25.0 or 23.0 cm, so the obstacle was submerged in the first case, whist it was emerged in the other two. 27 experimental runs (9 with submerged breakwater and 18 with emerged breakwater) were recorded, resulting from the combination of 3 different

[a] Corresponding author: ferraris@unica.it

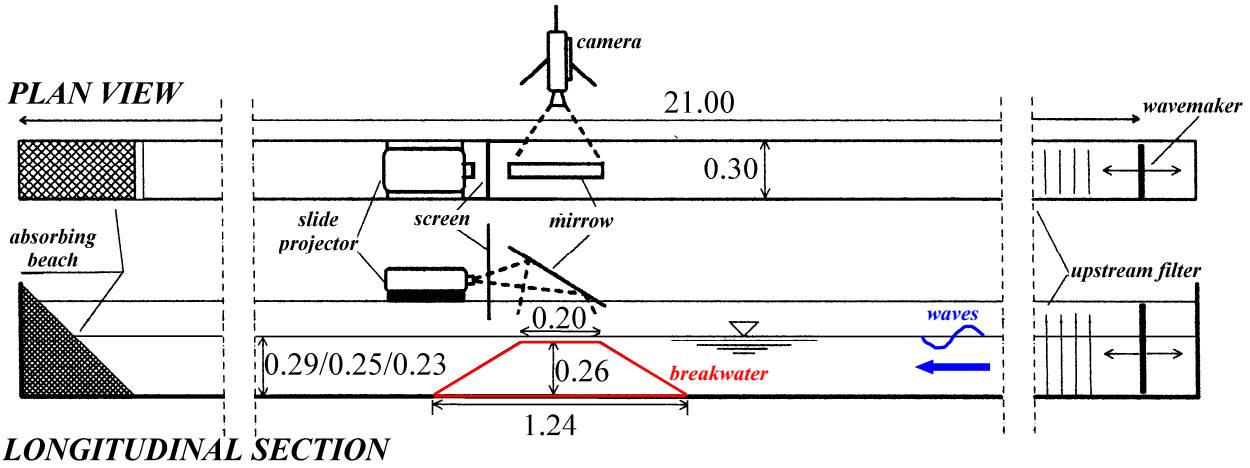

Figure 1. Experimental set-up (measures in m).

hydrostatic levels, wave periods T (0.8, 1.0 and 1.3 s) and amplitudes A. As breakwater and background were black, the working fluid was water seeded with non-buoyant particles and the area of interest was lighted with a light sheet, generated by two slide projectors, equipped with a black slide and a narrow vertical slit at its centre (see [7] for more details on this technique and on the characteristics of the light sheet). As a consequence, the water was clearly distinct from the background and the breakwater (see Figure 2) and the free surface can be identified as the interface between dark and lighted zones.

During the last years, various Image Analysis techniques have been developed by the staff of the DICAAR – University of Cagliari to measure concentrations ([7]) and velocities ([8], [9]) in a non-intrusive and continuous in space way: this gives the advantages of not modifying the flow inserting probes into it and of reducing the time spent in experiments, as the measures are obtained all over the investigation field. In order to develop and test a new Image Analysis technique able to estimate the wave motion transformations over a breakwater, experiments were recorded by a 3-CCD digital video camera, orthogonal to the light sheet, at the frequency of 25 images per second.

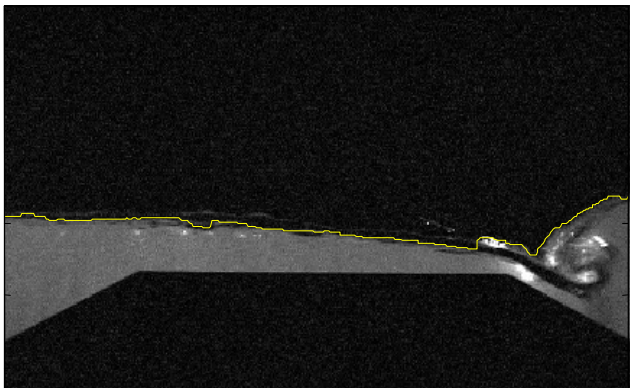

Figure 2. Example of free surface identification (yellow line): the weather side is on the right and the lee is side on the left.

The recorded images were digitalized at a 576x720 pixels resolution, then a median filter and afterwards a simple threshold segmentation were performed on them, with the target of identifying the free surface as the interface between water (white) from background (black). To avoid misleading (e.g., from small drops, small black areas in the lighted zone or in bright areas in the dark ones), the following procedure was employed:

1. each column in a given image was analyzed pixel by pixel, from the upper side of the image downwards, as far as a black/white interface was detected;
2. when a white pixel was detected, a certain number of successive pixels was checked;
3. if all of them were as well white, the first pixel was recognized as belonging to the free surface.

When the full image was elaborated and all the points of the free surface were found, another median filter was applied, to smooth the line representing free surface.

Following the described procedure, it is possible to identify the free surface at as many points as the horizontal resolution of the video-camera, also when the obstacle is emerged or with breaking waves. Consequently, this technique can identify the entire free surface, while traditional resistive probes are able to give information only in the points where they are used. Moreover, this method allows to define even a posteriori the number and the positions of the points to study. Eventually, this method works even in prohibitive situations for traditional resistive probes, as in the case of very shallow water above the breakwater or with breaking waves.

3 Results

As shown in Figure 1, the waves are generated by the wave-maker on the right side of the flume and they run from right to left, so on every figures the weather side is on the right and the lee is side on the left. Moreover, the origin of abscissa X is put in the middle of the obstacle longitudinal section; the origin of the wave height H is put at the hydrostatic level.

Two kind of analysis were mainly performed on the data, a statistical (on the wave mean height, the wave height variance, the wave mean height in phase, the wave height variance in phase and the probability density of the surface height.) and a spectral one (on the power spectral density, the fundamental frequency and the harmonic ones). Thanks to the above illustrated peculiarities of the

measurement technique, the analyses were performed with continuity all over the top of the breakwater, so describing the whole transformation of the waves.

Before coming into the data analysis, a brief description of the phenomena that develop when the wave train comes over the obstacle will be done.

3.1 Phenomenological description

When the breakwater is submerged (hydrostatic level of 29.0 cm), upstream the obstacle a wave depression develops with the so-called plunging profile: it has the shape of a curl (see the right side of Figure 2) that grows up and then dives into the wave basis. This is the so-called wave breaking, that happens over the breakwater weather side, causing a strong turbulence with a consequent energy dissipation. In the experiments with wave period of 0.8 s, the profile is of surging type, which is characterized by a uniformly decreasing energy.

When the breakwater is emerged (hydrostatic level of 25.0 and 23.0 cm), the wave-breaking never happens and the water overflows the breakwater sliding on it, with no vortices on the weather side, while a hydraulic jump behaves on the lee side.

3.2 Statistical analysis

As before stated, the statistical analysis that will be shown hereafter are relative to the wave mean height (compared with hydrostatic level) and its variance, performed also phase by phase, and to the probability density of the free surface heights.

3.2.1 Overall mean value and variance of the wave height

In Figures 3 and 4, the wave mean heights H and the wave height variances σ^2 along the breakwater for the three experiments with submerged obstacle (hydrostatic level 29.0 cm) and period T of 0.8 s are plotted.

In Figure 3 the so-called wave set-up phenomenon is visible: downstream the breakwater, the water flow from weather side to lee one (that is closed) causes a raising of the free surface above the hydrostatic level. Upstream the breakwater, the phenomenon of the wave set-down is clear: the plunging profile behaviour determines a decreasing of the free surface under the hydrostatic level. Wave set-up and wave set-down are so accurately detected by the technique. Moreover, Figure 3 shows that both wave set-up and set-down tend to grow for increasing values of the wave amplitude A. From the comparison of Figure 3 with Figure 5 (same hydrostatic level but a different period T of 1.0 s), it is clear that wave set-up and set-down also tend to grow for increasing values of T.

In Figure 4 the wave height variance σ^2 is shown. σ^2 is proportional to A^2 and to the turbulence intensity, so the upstream peak, visible for all the amplitudes, points out the location X of the wave breaking: downstream this peak, the variance decreases almost uniformly, indicating that the profile is of plunging type. the wave height variance σ^2 tends to grow for increasing values of the wave amplitude A. From the comparison of Fig. 4 with Fig. 6 (same hydrostatic level but T = 1.0 s), it is clear that σ^2 tends to grow for increasing values of T.

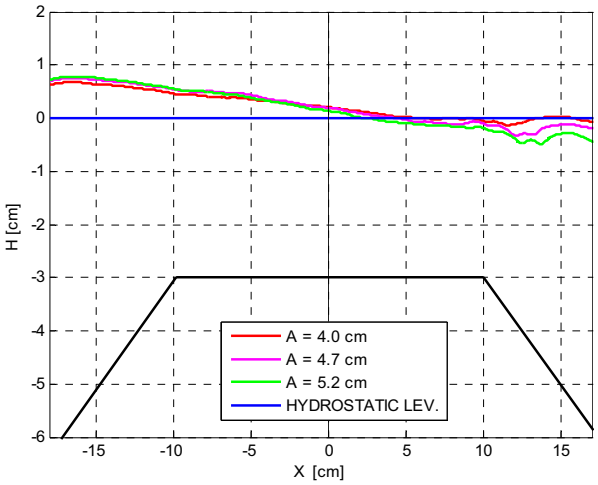

Figure 3. Wave mean height H along the breakwater for the runs with hydrostatic level of 29.0 cm, period T = 0.8 s and amplitude A of 4.0, 4.7 and 5.2 cm.

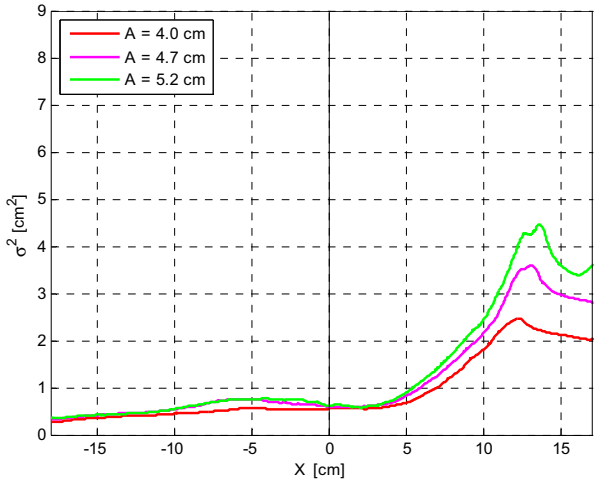

Figure 4. Wave height variance σ^2 along the breakwater for the same runs of Figure 3.

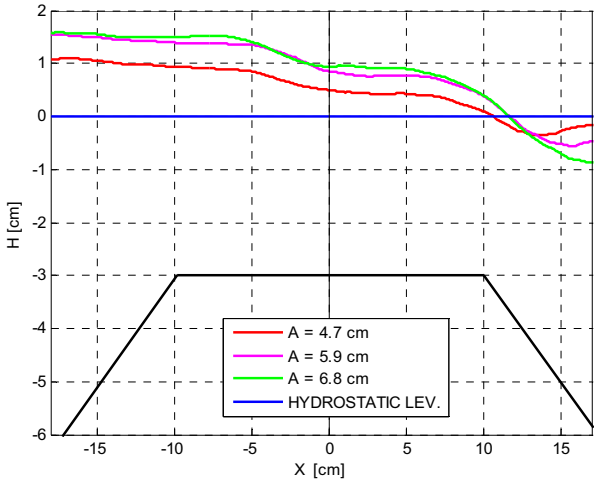

Figure 5. Wave mean height H along the breakwater for the runs with hydrostatic level 29.0 cm, period T = 1.0 s and amplitude A of 4.7, 5.9 and 6.8 cm.

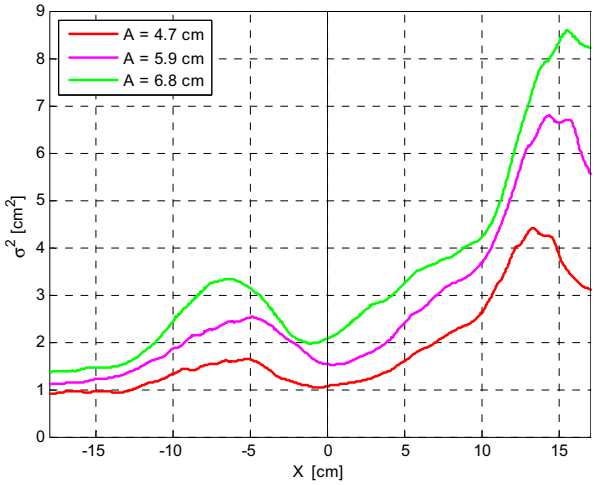

Figure 6. Wave height variance σ^2 along the breakwater for the same runs of Figure 5.

In Figure 6, there is instead a minimum value of σ^2 (in the middle of the breakwater) followed by another peak: the minimum value indicates the location X where the waves spill over themselves after the breaking, the following peak shows the consequent increase of the turbulence.

In Figures 7 and 8, the wave mean heights H and the wave height variances σ^2 along the breakwater for three of the runs with submerged breakwater (hydrostatic level 25.0 cm) and period T of 0.8 s are plotted. σ^2 in experiments with emerged breakwater has values that are very much lower than in ones with submerged breakwater, because there is not a breaking wave but only a raising followed by a regular decreasing of its height H. As a matter of fact, when the breakwater is emerged the water overtopping is just a slipping on the upper part of the breakwater, with a following hydraulic jump, visible in Figure 7. In this figure it is possible to note also that, near the downstream edge of the breakwater, the water height H is almost zero: these areas will be called "dry zones". A dry zone appears when the wave, during the overtopping of the breakwater, looses almost entirely its energy. The dry time DT represents how long, during a run,

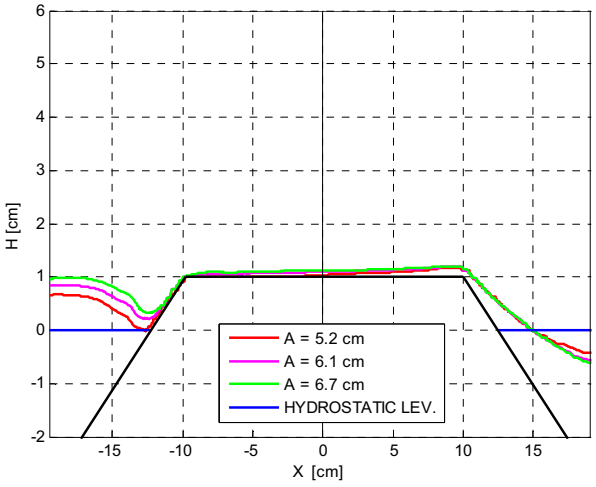

Figure 7. Wave mean height H along the breakwater for the runs with hydrostatic level of 25.0 cm, period T = 0.8 s and amplitude A of 5.2, 6.1 and 6.7 cm.

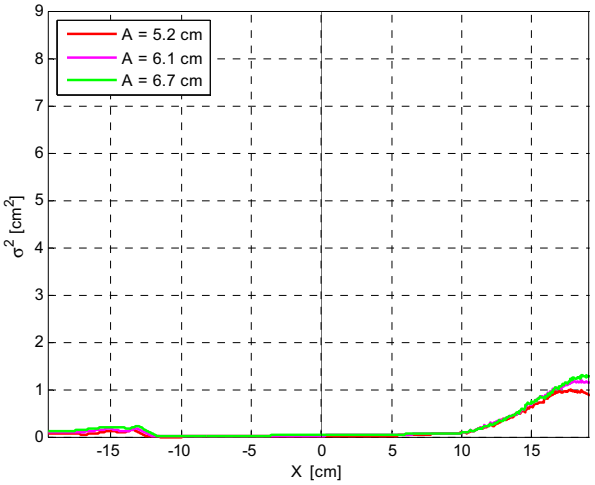

Figure 8. Wave height variance σ^2 along the breakwater for the same runs of Figure 7.

each part of the breakwater is a dry zone (i.e., how long each X experiences H ≅ 0 cm). In Figure 9 and 10, the dry time DT is plotted along the breakwater for the runs with hydrostatic level 25.0 and 23.0 cm.

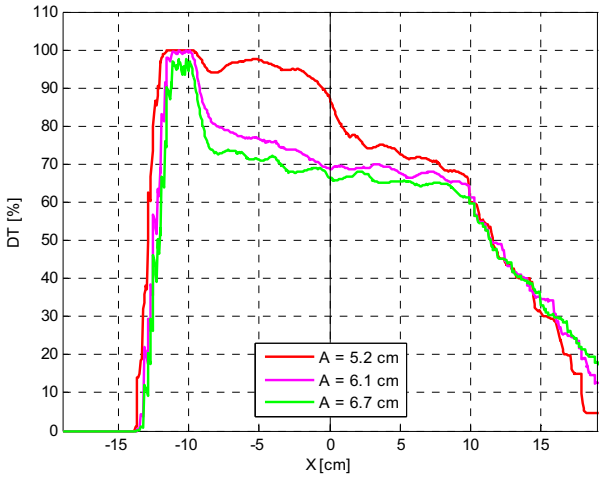

Figure 9. Dry time percentage DT along the breakwater for the runs with hydrostatic level of 25.0 cm, period T = 0.8 s and amplitude A of 5.2, 6.1 and 6.7 cm.

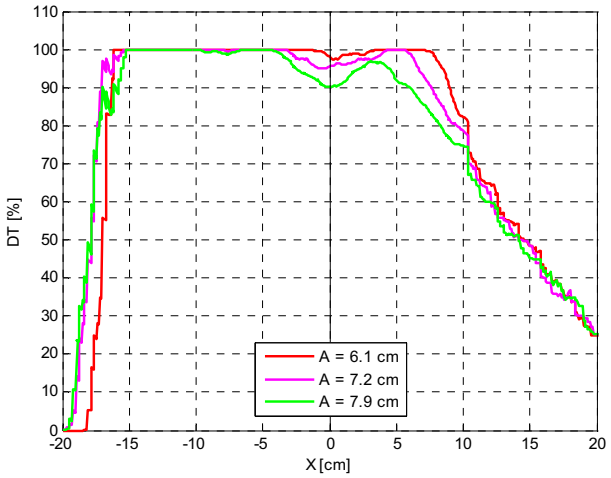

Figure 10. Dry time percentage DT along the breakwater for the runs with hydrostatic level of 23.0 cm, period T = 0.8 s and amplitude A of 6.1, 7.2 and 7.9 cm.

DT has a maximum on the downstream edge (Figure 9); moving downstream, DT tends to zero because H is always non zero in the lee zone of the breakwater. In the upstream breakwater edge, DT is non zero because the wave rundown makes the free surface go under hydrostatic level, leaving a zone of the breakwater uncovered. Comparing Figure 9 with Figure 10, it is possible to note that the dry zones and the dry time percentage DT increase with decreasing hydrostatic level, wave amplitude A and period T.

3.2.2 Mean value and variance of the wave height phase by phase

As already stated, the mean H and the variance σ^2 of the wave heights have been analyzed also phase by phase, in order, in particular, to highlight how σ^2 varies during the wave transit and transformation. In Figures from 11 to 14, four phases of the mean wave for the run with hydrostatic level 29.0 cm (submerged breakwater), T = 0.8 and A = 4.0 cm; above the wave mean height H in phase, compared with the mean one and the hydrostatic level; below, the variance σ^2 in phase.

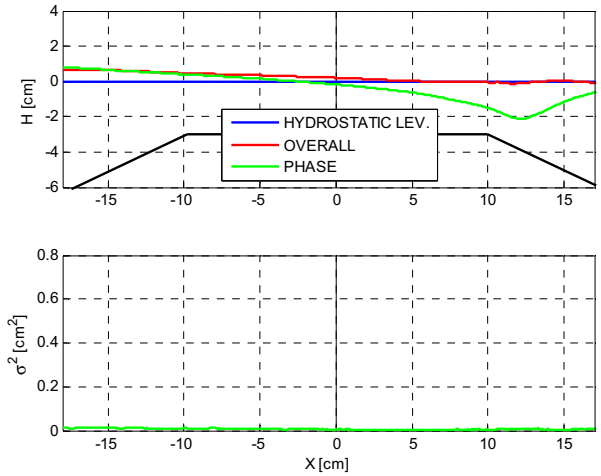

Figure 11. Wave mean height H (above) and variance σ^2 (below) along the breakwater at phase 1/5 for the run with hydrostatic level 29.0 cm, T = 0.8 s and A = 4.0 cm.

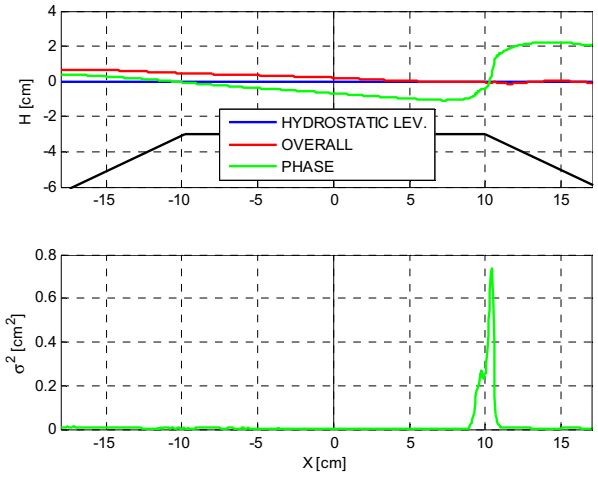

Figure 12. Wave mean height H (above) and variance σ^2 (below) along the breakwater at phase 2/5 for the same run of Figure 11.

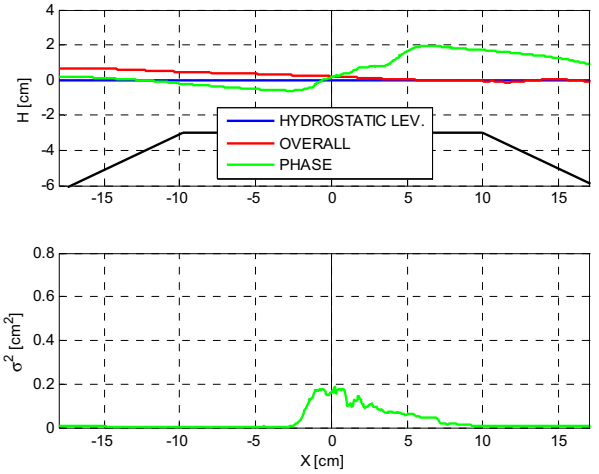

Figure 13. Wave mean height H (above) and variance σ^2 (below) along the breakwater at phase 3/5 for the same run of Figure 11.

.

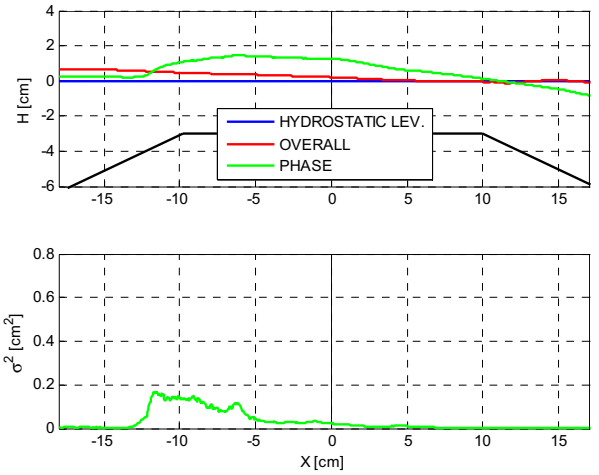

Figure 14. Wave mean height H (above) and variance σ^2 (below) along the breakwater at phase 4/5 for the same run of Figure 11.

During the wave set-down (Figure 11), the wave prepares for overtopping the breakwater, there is not yet any wave breaking or turbulence, so the variance σ^2 is almost zero along all the investigation area. When the wave breaks (Figure 12), the variance σ^2 reaches its maximum value, pointing out that the wave breaks, with a sudden increase of the turbulence level. This peak of variance σ^2 then moves along the obstacle, carried by the wave, with lower values.

The same analysis is shown in Figures from 15 to 18, for the run with hydrostatic level 25.0 cm (emerged breakwater), T = 0.8 and A = 6.1 cm. In the experiments with emerged breakwater, two peaks of variance σ^2 can be spotted: they have lower values than the one experienced with the submerged breakwater. The peak upstream the breakwater is caused by the wave that prepares for the overtopping of the obstacle; the peak downstream the breakwater point out the turbulence generated by the hydraulic jump that develops there. The peaks of variance σ^2 tend to increase with increasing values of amplitude A and period T, both in the case with submerged and emerged breakwater.

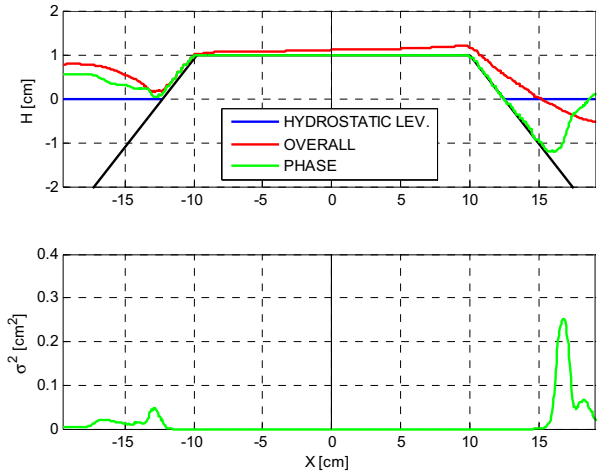

Figure 15. Wave mean height H (above) and variance σ^2 (below) along the breakwater at phase 1/5 for the run with hydrostatic level 25.0 cm, T = 0.8 s and A = 6.1 cm.

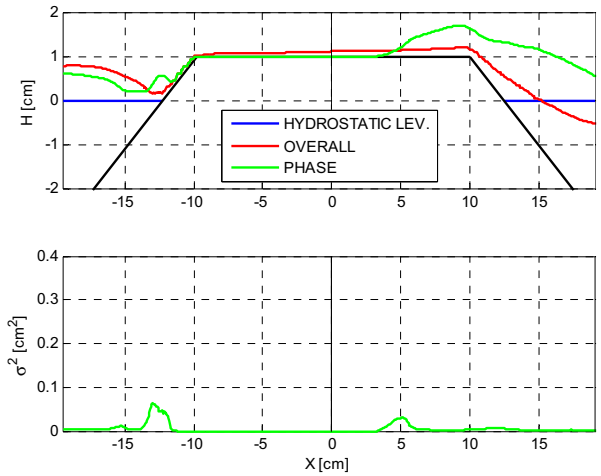

Figure 16. Wave mean height H (above) and variance σ^2 (below) at phase 2/5 for the same run of Figure 15.

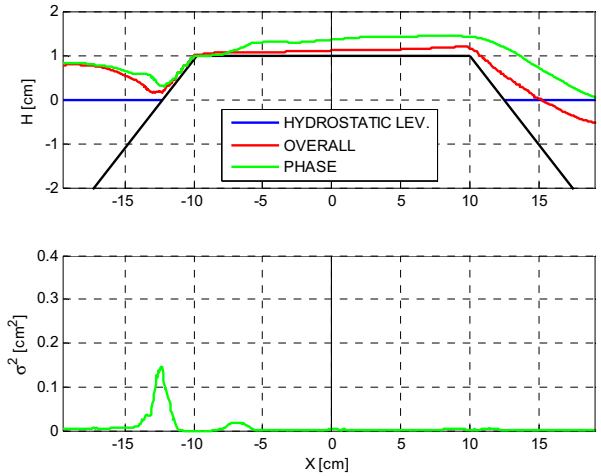

Figure 17. Wave mean height H (above) and variance σ^2 (below) at phase 3/5 for the same run of Figure 15.

3.2.3 Probability density of the free surface heights

As shown before, the Image Analysis technique employed in this work allows to perform measurements and, so, to analyse every single point in the investigation area.

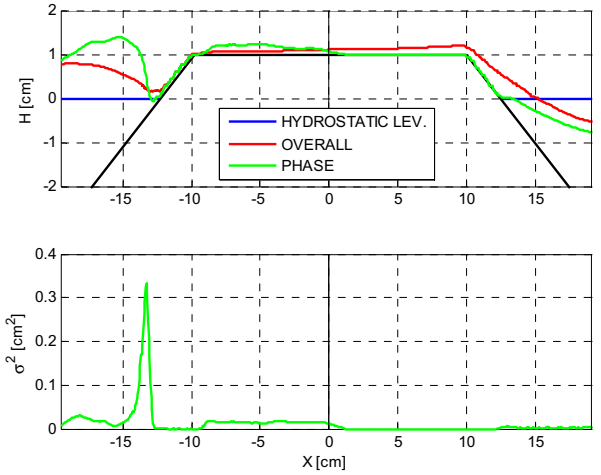

Figure 18. Wave mean height H (above) and variance σ^2 (below) along the breakwater at phase 4/5 for the same run of Figure 15.

We have taken advantage from this feature of the technique was to compute the Probability Density Function (PDF) of the wave heights H for the whole free surface, highlighting some wave characteristics that cannot be spotted from a simple statistical analysis of the wave mean height.

In Figure 19 the Probability Density Function (PDF) of the free surface height H in all the investigation area is shown for a hydrostatic level of 29.0 cm (breakwater submergence of 3.0 cm), with a wave amplitude A = 4.7 cm and a period T = 1.0 s; colours represent the probability density that the wave free surface was in a particular location (dark blue for a zero value, dark red for a high value). The point where the wave breaks corresponds to the upstream depression (X ≅ 0 cm). The net of blue lines visible on the right side of Figure 19 is due to the fact that the wave frequency F (1.0 Hz, being the inverse of the wave period T) is an exact divisor of the camera acquisition rate (25.0 Hz), so there is a high probability for the free surface to be in the same position after a fixed number of frames. The vertical lines of the net identify the positions occupied by the advancing wave front, while the horizontal lines identify the positions of the wave free surface during its withdrawal, up to the point where a new wave breaks. A multi-modal probability distribution is also apparent, describing the typical wave behaviour, both during the set-up (pointed out by red U in Figure 19) and set-down (white D) phases. Moreover, the occurrence of the blocking phenomenon is clear when looking at the upper boundary of the PDF: the wave behaves with time always in the same way, with blocked phases.

In Figure 20, the same analysis is performed on a run with an emerged breakwater: in this case, the Probability Density Function (PDF) of the free surface height H in all the investigation area is shown for a hydrostatic level of 25.0 cm, with a wave amplitude A = 5.6 cm and a period T = 1.0 s. In the PDF analysis with an emerged breakwater, the instants in which that point is in dry time are not taken into account in the statistics. When the obstacle is emerged, the above cited dry zones, the

upstream raising and the downstream hydraulic jump are easily spotted.

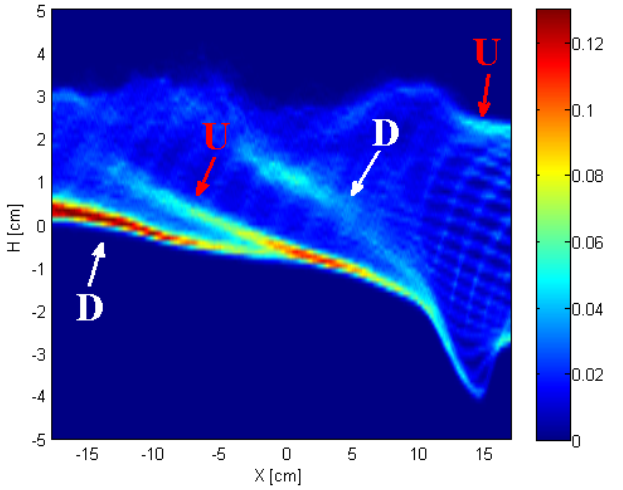

Figure 19. Probability Density Function (PDF) of the wave height H in the investigation area for the run with hydrostatic level 29.0 cm, T = 1.0 s and A = 4.7 cm.

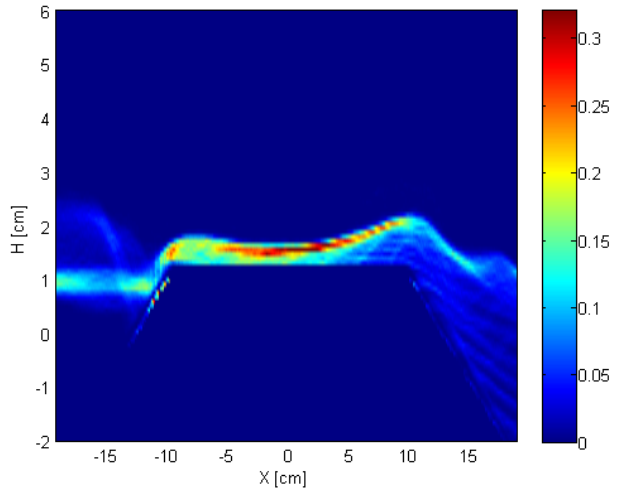

Figure 20. Probability Density Function (PDF) of the wave height H in the investigation area for the run with hydrostatic level 25.0 cm, T = 1.0 s and A = 5.6 cm.

3.3 Power spectral analysis

When a regular wave train, generated by the wave-maker, interact with the breakwater, it looses its linearity and, from this point downstream, it is no longer regular: in this case the waves can be studied with a power spectral analysis. The power spectral analysis performed continuously above the breakwater allows to assess the power density attenuation that each section of the breakwater causes. In Figure 21, 24 and 25 the log10 of the power spectral density PD (colours) is plotted in a chart with frequency F versus X.; log10 is employed to better highlight amounts of energy also very little. When the wave passes over the breakwater, there is an energy transfer from the fundamental frequency (the one carrying the highest fraction of energy) to the harmonic ones, multiples of the fundamental, so the wave energy decreases from the fundamental frequency to the harmonic ones, as it clearly visible in Figure 21. Indeed the highest harmonics are particularly noticeable only on the breakwater upstream side, showing the wave looses its linearity mainly over the breakwater, consistently with Ohyama and Nadaoka findings [10]. Moreover, this analysis confirms that the lower harmonic is the first to be generated, followed by all the other ones. In Figure 22, the fundamental frequency and the first harmonic are plotted along the breakwater: this plot allows to highlight that the greatest fraction of energy is dissipated on the upstream side of the breakwater which is, consequently, the most efficient from the energy dissipation point of view. Thanks to the technique, this density power dissipation can be quantified in of more than ten times of the initial value. Looking at Figure 23, where the fundamental frequencies of the three runs with hydrostatic level equals to 29.0 cm and period to 0.8 cm are plotted, it is possible to understand that the dissipation increases with increasing wave amplitude A.

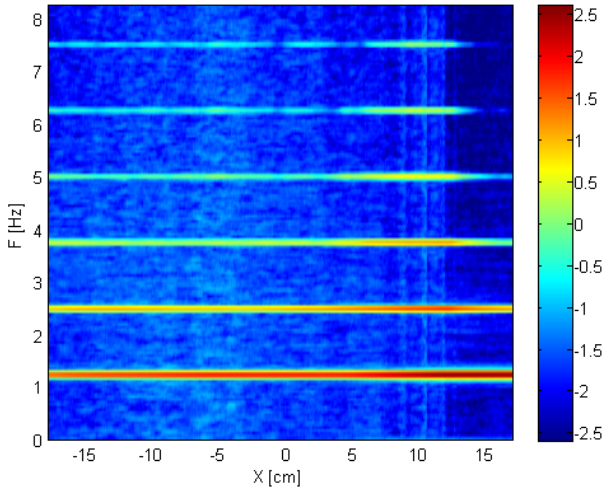

Figure 21. Log 10 of the Power Spectral Density (cm^2 s^2), for the various frequency F, along the breakwater for the run with hydrostatic level 29.0 cm, T = 0.8 s and A = 4.0 cm.

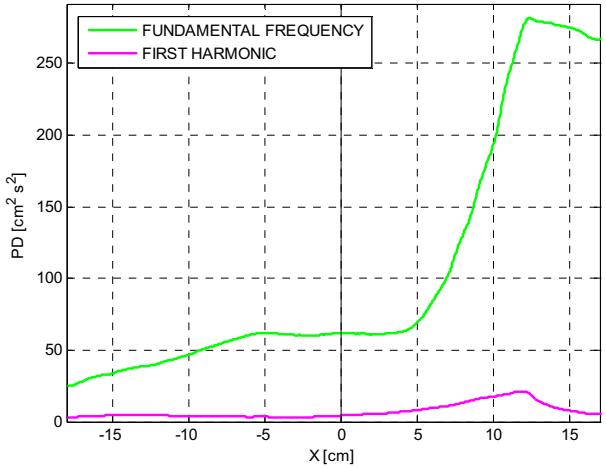

Figure 22. Power spectral density (cm^2 s^2) of fundamental frequency and first harmonic for the same run of figure 21.

In Figure 24, the previously mentioned blocking phenomenon is visible for the highest harmonics, as some of the harmonics do not have a constant energy along X but zones of higher energy are alternate to other of lower one. When, as in Figure 25, the breakwater is emerged, the power dissipation is almost complete already on the

breakwater upstream side and a dry zone, with zero energy, arises (dark blue vertical stripe).

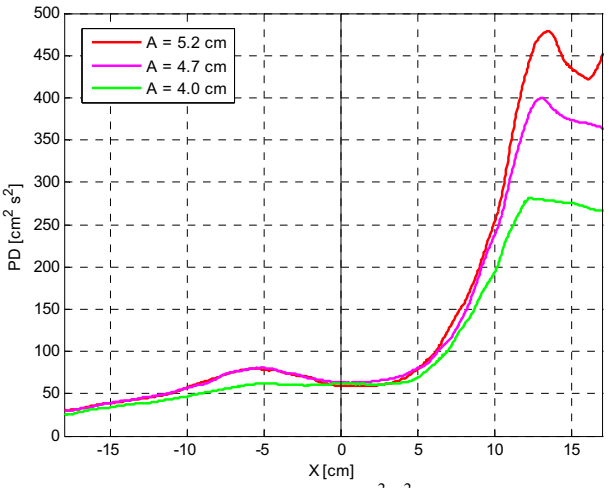

Figure 23. Power spectral density (cm^2 s^2) of the fundamental frequencies for the three runs with hydrostatic level 29.0 cm and period 0.8 s.

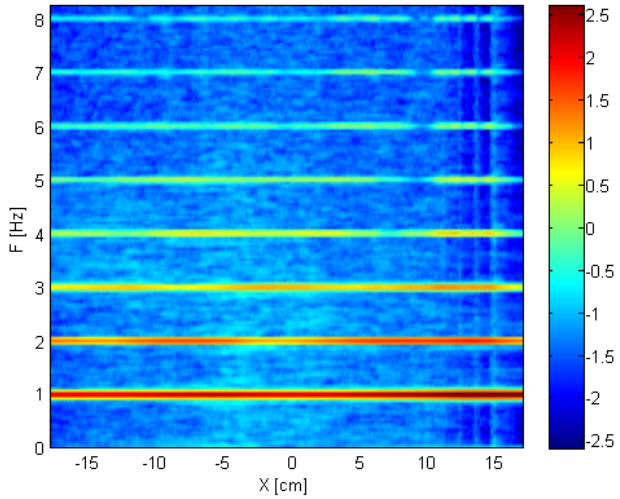

Figure 24. Log 10 of the Power Spectral Density (cm^2 s^2), for the various frequency F, along the breakwater for the run with hydrostatic level 29.0 cm, T = 1.0 s and A = 4.7.

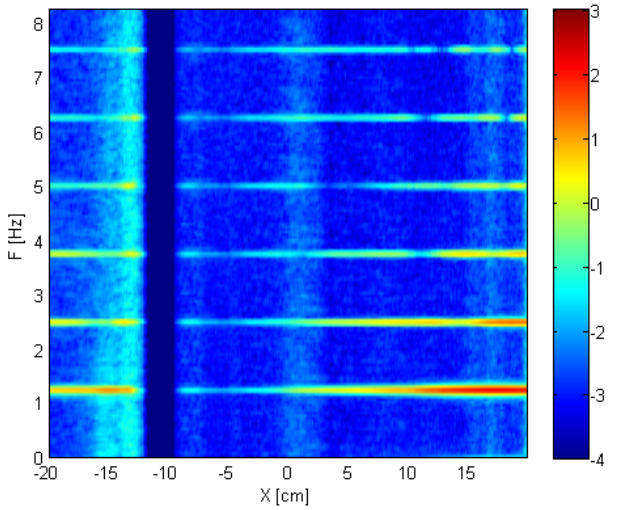

Figure 25. Log 10 of the Power Spectral Density (cm^2 s^2), for the various frequency F, along the breakwater for the run with hydrostatic level 25.0 cm, T = 0.8 s and A = 5.2 cm.

Downstream the dry zone, the wave slips down the breakwater recovering energy and forming a hydraulic jump: the energy is redistributed more uniformly among the various frequencies (pale blue area on the left of the dry zone) and the flow sharp separation in frequencies multiple of the fundamental is no more present.

4 Conclusions

A non-intrusive and continuous-in-space technique, based on Image Analysis, has been developed to overcome the limits of traditional resistive probes, usually employed to investigate wave transformation caused by a breakwater. This technique has proved to properly work also in situations that would be prohibitive for traditional probes (e.g. very shallow water and/or breaking waves) and has allowed performing quantitative analyses with continuity all over the investigation area. The wave transformations above a trapezoidal breakwater, both emerged and submerged, were studied in the laboratory by means of this method. The statistical analysis of wave height has allowed the observation of wave breaking and the measure of set-up and set-down: they increase with increasing wave amplitudes and periods. The measure of the variance of the wave height has allowed to identify if (and, in case, where) the wave breaks: also the variance increases with increasing wave amplitudes and periods. Dry zones (where the water level is almost zero) has been detected and quantified. The blocking phenomenon was spotted thanks to a power density analysis. The Power spectra have been also measured: they are able to quantitatively describe both the energy dissipation (and where it occurs above the breakwater) and the wave non-linear transformations from the weather to lee side of the breakwater, with the resulting energy transfer among the frequencies. The quantities measured thanks to this technique can be supply useful information for design purposes.

References

1. N.G. Rangel-Buitrago, G. Anfuso, A.T. Williams, A.T., Ocean Coast Manage **114**, 129-144 (2015).
2. M.E. McCormick, R.C. Murtha, J. Steinmetz, Mar Technol Soc J **47** (4), 187-192 (2013).
3. T. Sawaragi, *Proceedings of 23° International Conference on Coastal Engineering*, 351-368 (1992).
4. C.K. Ting Francis, K. Young-Ki, Coast Eng **24**, 23-49 (1994).
5. M. Di Risio, I. Lisi, G.M. Beltramiand, P. De Girolamo, Ocean Eng **37** (8-9), 777-789 (2010).
6. S. Ferrari, G. Querzoli, EPJ Web of Conferences **92**, 02018 (2015).
7. S. Ferrari, G. Querzoli, J Hydr Res **48**(5), 632-640 (2010).
8. L.A. Besalduch, M.G. Badas, S. Ferrari, G. Querzoli, EPJ Web of Conferences **67**, 02007 (2014).
9. L.A. Besalduch, M.G. Badas, S. Ferrari, G. Querzoli, EPJ Web of Conferences **45**, 01012 (2013).
10. T. Ohyama, K. Nadaoka, Coast Eng **24**, 1-22 (1994).